Environ. Sci. Technol. **2007**, *41,* 3347−3353

Tubular Membrane Cathodes for Scalable Power Generation in Microbial Fuel Cells

YI ZUO, SHAOAN CHENG, DOUG CALL, AND BRUCE E. LOGAN*

Department of Civil and Environmental Engineering, The Pennsylvania State University, University Park, Pennsylvania 16802

One of the greatest challenges for using microbial fuel cells (MFCs) for wastewater treatment is creating a scalable architecture that provides large surface areas for oxygen reduction at the cathode and bacteria growth on the anode. We demonstrate here a scalable cathode concept by showing that a tubular ultrafiltration membrane with a conductive graphite coating and a nonprecious metal catalyst (CoTMPP) can be used to produce power in an MFC. Using a carbon paper anode (surface area $A_{an} = 7$ cm^2, surface area per reactor volume $A_{an,s} = 25$ m^2/m^3), an MFC with two 3-cm tube cathodes ($A_{cat} = 27$ cm^2, $A_{cat,s} = 84$ m^2/m^3) generated up to 8.8 W/m^3 (403 mW/m^2) using glucose [0.8 g/L in a 50 mM phosphate buffer solution (PBS)], which was only slightly less than that produced using a carbon paper cathode with a Pt catalyst (9.9 W/m^3, 394 mW/m^2; $A_{cat} = 7$ cm^2, $A_{cat,s} = 25$ m^2/m^3). Coulombic efficiencies (CEs) with carbon paper anodes were 25−40% with tube cathodes (CoTMPP), compared to 7−19% with a carbon paper cathode. When a high-surface-area graphite brush anode was used ($A_{an} = 2235$ cm^2, $A_{an,s} = 7700$ m^2/m^3) with two tube cathodes placed inside the reactor ($A_{cat} = 27$ cm^2, $A_{cat,s} = 93$ m^2/m^3), the MFC produced 17.7 W/m^3 with a CE = 70−74% (200 mM PBS). Further increases in the surface area of the tube cathodes to 54 cm^2 (120 m^2/m^3) increased the total power output (from 0.51 to 0.83 mW), but the increase in volume resulted in a constant volumetric power density (∼18 W/m^3). These results demonstrate that an MFC design using tubular cathodes coated with nonprecious metal catalysts, and brush anodes, is a promising architecture that is intrinsically scalable for creating larger systems. Further increases in power output will be possible through the development of cathodes with lower internal resistances.

Introduction

A microbial fuel cell (MFC) is a promising technology for wastewater treatment because it can produce electricity at the same time that the biodegradable organic matter is removed (*1*−*3*). In an MFC system, the characteristics of the cathode can substantially affect electricity generation (*4*−*6*). Various catholytes have been used in MFCs, including oxygen (*7*, *8*), ferricyanide (*9*−*11*), and metal oxides such as MnO_2 (*12*). However, oxygen is considered as the most suitable electron acceptor for practical MFC systems because it is free and its use is sustainable (*13*). Exposing one side of the cathode to air (air cathode) has significantly improved power production, compared to dissolving air in the cathode electrolyte (aqueous cathode) (*2*). In a single-chamber MFC containing an air cathode, the maximum power density was 262 mW/m^2 (6.6 W/m^3; Coulombic efficiency (CE) = 40−55%) using glucose when a cation exchange membrane (Nafion) was hot-pressed onto the cathode (*7*). Removing the Nafion membrane increased the power density to 494 mW/m^2 (12.4 W/m^3), but decreased the CE to 9−12% as a result of greater oxygen diffusion into the reactor (*7*). Adding a diffusion layer to the air side of the cathode increased the CE to 20−27%, and also increased power production to 766 mW/m^2 (19.2 W/m^3) (*5*).

One of the biggest challenges for developing large-scale MFCs is a method to produce a scalable air cathode architecture that is cost-effective. Tubular cathodes can provide high surface area to volume ratios, but there have been few investigations with this type of architecture in MFCs. In one system a tubular cathode was made by hot-pressing carbon cloth containing a Pt catalyst to a Nafion membrane, and then wrapping the material around a porous plastic tube. This approach generated 26 mW/m^2 (1.6 W/m^3) with domestic wastewater as a substrate (*14*). Two other approaches have been tried, but both used ferricyanide as a catholyte rather than oxygen. In one system the cylindrical cathode made of a woven graphite mat was placed on a cation exchange membrane and wrapped around the anode so that the ferricyanide solution flowed down over the outside of the cathode (*15*). In the second system the ferricyanide solution was pumped through a cation exchange membrane formed tube, with graphite granules packed into the tube as the cathode material, and then the tube was placed in a concentric manner inside a column containing a bed of graphite granules that served as the anode (*16*). While these two studies with ferricyanide have achieved greater power production than systems using oxygen, it is generally accepted that the use of ferricyanide is unsustainable and thus not a practical approach for MFC applications such as wastewater treatment (*2*).

Another limitation of existing air cathode systems is the catalyst. Platinum is widely used in laboratory systems for air cathodes to catalyze oxygen reduction, but it is also considered to be impractical for large scale systems due to its high cost. Co-tetra-methyl phenylporphyrin (CoTMPP) and iron phthalocyanine (FePc) have recently been shown to be suitable alternatives to Pt in MFCs (*17*, *18*).

In this study, we demonstrate a new approach for cathode design based on converting tubular ultrafiltration membranes into MFC cathodes. Instead of joining carbon cloth or paper to a membrane or using graphite granules, we made the membrane itself the cathode by coating it with a high graphite content paint. We then added CoTMPP to the painted surface to catalyze the reduction of oxygen to water. The use of a tube cathode permits passive transport of oxygen to the catalyst, while at the same time limiting water loss due to the low water membrane permeability but allowing proton transport to the air-facing side of the membrane. The performance of various types of tube cathodes was investigated using conventional carbon paper anodes and newly developed graphite brush anodes described in a companion paper in this issue (*19*). We compared the performance of these systems to that of a commercial carbon paper cathode in terms of power and CE, and examined different locations of the catalyst (inside and outside of the tube), configurations

* Corresponding author phone: 814-863-7908; fax: 814-863-7304; e-mail: blogan@psu.edu.

10.1021/es0627601 CCC: $37.00
Published on Web 03/21/2007

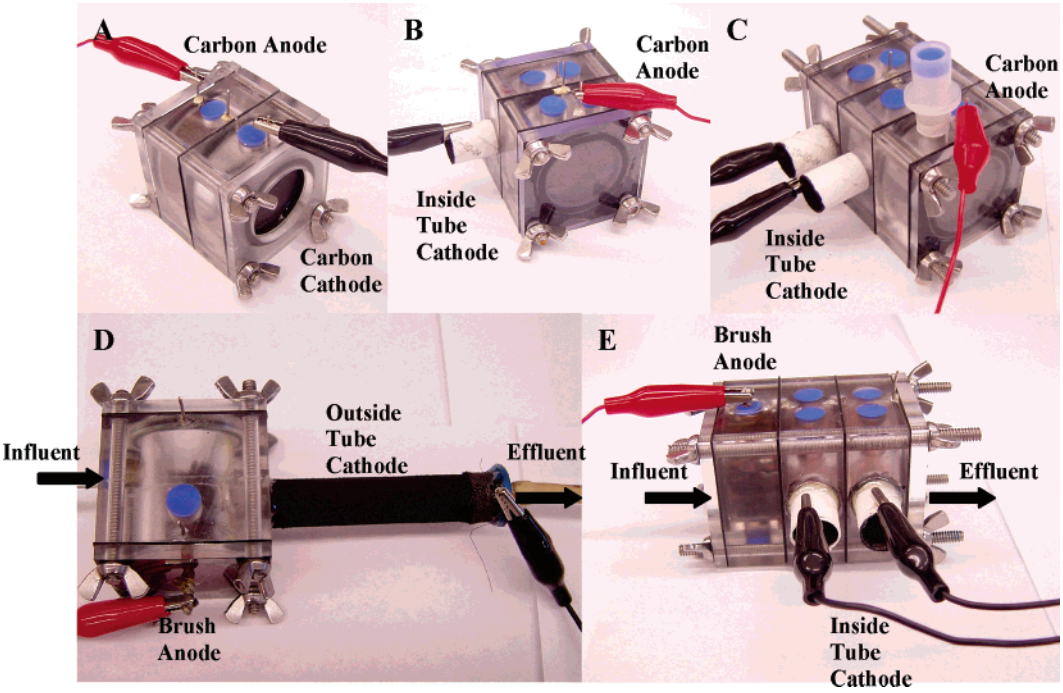

FIGURE 1. Different MFC configurations. Carbon paper anode MFCs with (A) Pt on a carbon paper cathode (C-CPt-I), (B) 3-cm tube-cathode (C-T_1Co-I or C-T_1C-I), and (C) two 3-cm tube-cathodes (C-T_2Co-I). Brush anode MFCs with (D) a single 6-cm long tube-cathode outside the reactor (B-T_2Co-O), and (E) two 3-cm tube-cathodes placed inside the MFC (B-T_2Co-I).

of the cathode (inside and outside the reactor), and operation mode of the reactor (fed batch and continuous flow).

Materials and Methods

Cathode Preparation. An ultrafiltration hydrophilic tubular membrane (a polysulfone membrane on a composite polyester carrier) with an inner diameter of 14.4 mm (B0125, X-FLOW) and wall thickness of 0.6 mm was used as the tube cathode. The tubes were cut to lengths of 3, 6, or 12 cm (equal to surface areas of 13.5, 27, and 54 cm^2) and then were coated with a proprietary graphite paint two times (ELC E34 Semi-Colloidal, Superior Graphite Co.). Co-tetra-methyl phenylporphyrin (CoTMPP) was used as the cathode catalyst unless indicated otherwise. A CoTMPP/carbon mixture (20% CoTMPP) was prepared as previously described (*17*) and mixed with a 5% Nafion solution to form a paste (7 μL of Nafion per mg of CoTMPP/C catalyst). The paste was then applied to the air-facing surfaces of all tube cathodes (~0.5 mg/cm^2 CoTMPP loading). In some tests a commercial carbon paper cathode containing Pt (0.35 mg/cm^2 of Pt catalyst, water proofed paper, E-Tek; $A_{cat} = 7$ cm^2) was used with the catalyst facing the water solution. A 3-cm tube cathode containing only graphite paint was prepared as a noncatalyst control.

Anode Preparation. The anode electrode was either a piece of plain Toray carbon paper (without wet proofing; E-Tek; $A_{an} = 7$ cm^2) or a plain graphite fiber brush (25 mm diameter × 25 mm length; fiber type: PANEX 33 160K, ZOLTEK) with an estimated surface area of 2235 cm^2 (95% porosity) (*19*).

Tube Cathode Reactors with Carbon Paper Anodes. In order to distinguish among different types of reactors, we designated each reactor configuration using the notation of X-YZ-J, where: X = anode material (C = carbon paper, B = graphite brush); Y = cathode material (C = carbon paper, T_n = number of 3-cm lengths of tube cathodes, where $n = 1-4$); Z = catalyst (Pt = platinum; Co = CoTMPP; C = carbon without catalysts); and J = cathode configuration (I = inside reactor, O = outside reactor) (Figure 1). Three single-chamber carbon paper anode (C) MFCs were constructed with the tube-cathodes located inside (I) cylindrical chambered reactors (4 or 6 cm length × 3 cm diameter) (Table 1). Two of these reactors were constructed with CoTMPP coated tube-cathodes (TCo). One had a single 3-cm tube (C-T_1Co-I; 4-cm chamber), for a total cathode surface area of $A_{cat} = 13.5$ cm^2, and a surface area normalized to the reactor volume of $A_{cat,s} = 59$ m^2/m^3, while the other had two 3-cm tubes connected by a wire (C-T_2Co-I; 6-cm chamber; $A_{cat} = 27$ cm^2, $A_{cat,s} = 84$ m^2/m^3) (Figure 1B and C). The third system contained a single 3-cm tube-cathode without any catalyst (C-T_1C-I; 4-cm chamber; $A_{cat} = 13.5$ cm^2, $A_{cat,s} = 59$ m^2/m^3) (Figure 1B). Each cathode tube was inserted through the center of a single 2-cm-long slice of the chamber, with the carbon paper anode placed at an opposite side of another 2-cm-long slice. The CoTMPP catalyst layer was coated on the inside of these tubes (membrane side) and faced air. A single-chamber cube MFC of same type used in previous studies (*7*) was also tested by using a carbon paper anode and a carbon paper cathode with a Pt catalyst (C-CPt-I; $A_{cat} = 7$ cm^2, $A_{cat,s} = 25$ m^2/m^3), with the electrodes placed at opposite sides of the chamber (4 cm length × 3 cm diameter) (Figure 1A).

Tube Cathode Reactors with Brush Anodes. Two different brush anode (B) MFC configurations were tested with tube cathodes containing a CoTMPP catalyst (TCo): a cylindrical chambered MFC (6 cm long × 3 cm diameter) with tubes inside (I) the reactor (B-T_2Co-I); and the same type of reactor (4 cm × 3 cm diameter), but with the tube cathode placed outside (O) the reactor (B-T_2Co-O) (Table 1). For the inside tube reactor, a graphite brush anode placed vertically in a 2-cm-long reactor slide, and two wire-connected tube cathodes each 3 cm long were inserted through adjacent 2-cm slices producing a 6-cm long reactor (B-T_2Co-I; $A_{cat} = 27$ cm^2, $A_{cat,s} = 93$ m^2/m^3) (Figure 1E). The catalyst was coated on the inside of the tube (membrane side) and faced the air. The MFC with the cathode tube placed outside of the cube reactor was constructed using a brush anode placed horizontally in the center of a 4-cm-long chamber, with a single 6-cm-long (2 × 3 cm) cathode tube extending from one side

TABLE 1. Electrode Types and Surface Areas, Ratios of Electrode Area to Volume, Volumes, Internal Resistances, Maximum Power Density Normalized to Anode Surface Area or Total Reactor Volume, and CEs for All Carbon Paper and Brush Anode MFC Batch Tests (See Text for Reactor Designation Codes)

anode material	cathode material	cathode catalyst	catalyst location	reactor designation	A_{an} (cm^2)	$A_{an,s}$ (m^2/m^3)	A_{cat} (cm^2)	$A_{cat,s}$ (m^2/m^3)	volume (mL)	R_{int} (Ω)	P_{max} (mW/m^2)[a]	P_{max} (W/m^3)	CE (%)
carbon paper	2 tubes (3 cm each)	CoTMPP	inside tube	C-T_2Co-I	7	22	27	84	32	89 ± 5	403 ± 33	8.8 ± 1.0	25−33
carbon paper	1 tube (3 cm each)	CoTMPP	inside tube	C-T_1Co-I	7	30	13.5	59	23	131 ± 5	306 ± 8	9.3 ± 0.3	31−40
carbon paper	1 tube (3 cm each)	none	inside tube	C-T_1C-I	7	30	13.5	59	23	131 ± 5	101 ± 2	3.1 ± 0.1	18−22
carbon paper	carbon paper	Pt	inside reactor	C-CPt-I	7	25	7	25	28	84 ± 1	394 ± 3	9.9 ± 0.1	7−19
graphite brush	2 tubes (3 cm each)	CoTMPP	inside tube	B-T_2Co-I	2235	7700	27	93	29	66 ± 1	*b*	17.7 ± 0.2	70−74
graphite brush	1 tube (6 cm)	CoTMPP	outside tube	B-T_2Co-O	2235	6200	27	75	36	85 ± 8	*b*	8.2 ± 0.2	52−58

[a] Normalized to projected surface area of planar anodes. [b] Not applicable.

of the chamber (B-T_2Co-O; $A_{cat} = 27$ cm^2, $A_{cat,s} = 75$ m^2/m^3) (Figure 1D). In this case, the catalyst was coated on the outside of the tube (supporting side of membrane) and faced the air.

To further investigate the effect of cathode surface area, additional 3-cm tube cathodes were added to the inside of the MFCs, with external wires connecting the tubes (B-T_3Co-I and B-T_4Co-I). For reactors with tubes outside the reactor, the tube length was increased to 12 (4 × 3) cm (B-T_4Co-O), producing a cathode surface area of 54 cm^2.

Start Up and Operation. All MFCs were inoculated with a 50:50 mixture of domestic wastewater (~300 mg COD/L) and glucose (0.8 g/L) in phosphate buffer solution (PBS, 50 mM; pH = 7.0) in a nutrient medium (*7*). After 2−3 repeated feeding cycles, only media (no wastewater) was added. Reactors were considered to be acclimated if the maximum voltage produced was repeatable for at least three batch cycles. Following these tests, brush anode reactors were switched to 200 mM PBS as solution conductivity has been shown to increase power generation (*20*, *21*). The medium in the reactor was refilled when the voltage dropped below ~20 mV (resistances of 40−500 Ω) or ~40 mV (1000−3000 Ω).

Reactors with brush anodes and tube cathodes placed inside or outside the reactor were also operated in continuous flow mode with a hydraulic retention time (HRT) of 24 h (total volume of reactor; the influent was fed from the anode side (Figure 1D and E) by using a micro-infusion pump (AVI micro 210A infusion pump, 3M), with the flow discharged from the cathode side. All experiments were performed at ≤30 °C.

Calculations and Measurements. The Voltage (*V*) outputs of all reactors were measured across a fixed external resistance (1000 Ω except as noted) using a data acquisition system (2700, Keithly, USA). Electrode potentials were measured using a multimeter (83 III, Fluke, UAS) and a reference electrode (Ag/AgCl; RE-5B, Bioanalytical systems, USA). Current ($I = V/R$), power ($P = IV$), and CE (based on the input glucose) were calculated as previously described (*22*). Power and current density were either normalized to the projected area of carbon paper anodes (m^2) or the total reactor volume (m^3). To obtain the polarization curve and power density curve as a function of current, external circuit resistances were varied from 40 to 3000 Ω. For batch tests, one resistor was used for a full cycle (at least 24 h) for at least two separate cycles, while for continuous flow tests at least 24 h was used for each resistor.

Internal resistance, R_{int}, was measured by electrochemical impedance spectroscopy (EIS) over a frequency range of 10^5 to 0.005 Hz with sinusoidal perturbation of 10 mV amplitude using a potentiostat (PC 4/750 potentiostat, Gamry Instrument Inc.) for carbon paper anode MFCs filled with a nutrient media containing 50 mM PBS and brush anode reactors using 200 mM PBS. The anode was used as the working electrode and the cathode was used as the counter and reference electrode as described previously (*23*).

The maximum rate of oxygen transfer through a tube cathode was determined by measuring oxygen accumulation in an uninoculated carbon paper anode MFC reactor containing a clean 3-cm tubular membrane (without any graphite/catalysts) and de-oxygenated deionized water. The effective oxygen mass transfer coefficient of *k* was determined as previously described (*5*) with a dissolved oxygen probe (Foxy-21G, Ocean Optics Inc., FL) placed at the center of the stirred reactor. The resistance of proton transport through the tubular membrane cathode was determined by measuring the internal resistance increase when adding this membrane material between two carbon electrodes in a two-chamber cube reactor as previously described (*24*). The membrane tube was sliced open, cut into a circular shape to produce a flat surface of 7 cm^2, and then placed in the middle of the reactor with carbon electrodes each spaced 2 cm from the membrane. The internal resistances of the reactor with the membrane ($R_{int,m+}$) and without any membrane ($R_{int,m-}$) were measured by EIS using a potentiostat. The proton transport resistivity (Ω·cm^2) of the tubular membrane was calculated as $(R_{int,m+} - R_{int,m-}) \times A_{mem}$.

COD concentrations of the reactor effluent were measured using standard methods (*25*).

Results

Power Production from Tube Reactors with Carbon Paper Anodes. Repeatable cycles of power production were rapidly generated after acclimation of all four carbon paper anode MFC reactors. Power density curves and polarization curves obtained by varying the external circuit resistances from 40 to 3000 Ω showed that the tube cathode MFC with two CoTMPP coated tubes (C-T_2Co-I; $A_{cat} = 27$ cm^2) produced power only somewhat less than that achieved with a carbon paper cathode with Pt catalyst (C-CPt-I; $A_{cat} = 7$ cm^2), with a maximum power density of 8.8 ± 1.0 W/m^3 (403 ± 33 mW/m^2, anode surface area) for the tube cathode system and 9.9 ± 0.1 W/m^3 (394 ± 3 mW/m^2) for the carbon paper cathode (both at $R_{ext} = 250$ Ω; Figure 2A). Decreasing the tube cathode area by 50% (C-T_1Co-I, $A_{cat} = 13.5$ cm^2) slightly affected the volumetric power density (9.3 ± 0.3 W/m^3; $R_{ext} = 250$ Ω) due to the reduced volume without the cathode, but reduced power by 24% on the basis of the anode surface area (306 ± 8 mW/m^2). In the absence of a catalyst, the tube reactor (C-T_1C-I, $A_{cat} = 13.5$ cm^2) produced much less power, or 3.1 ± 0.1 W/m^3 ($R_{ext} = 250$ Ω) (Figure 2A). The internal resistances of these four MFCs ranged from 84 to 131 Ω (Table 1).

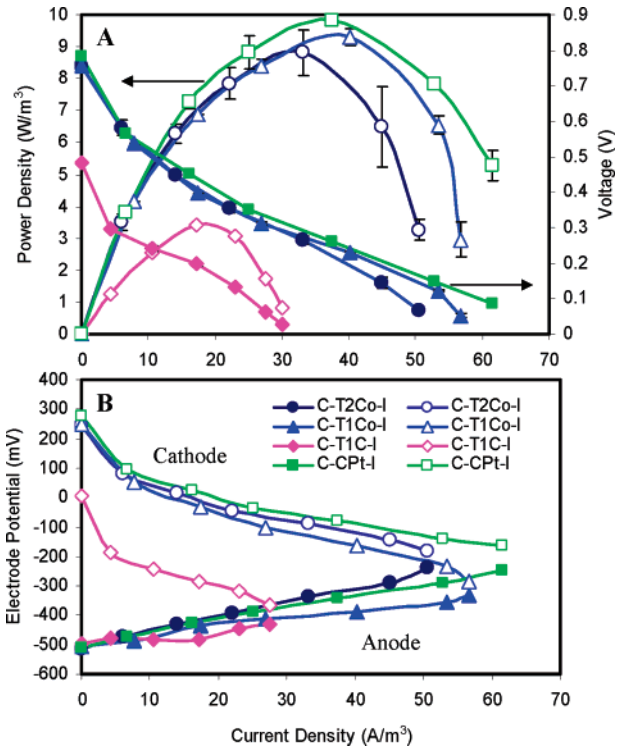

FIGURE 2. (A) Power density (open symbols), voltage (filled symbols), and (B) electrode potentials (cathode open symbols, anode filled symbols) as a function of current density (normalized to total reactor volume) obtained by varying the external circuit resistance (40−3000 Ω) for carbon paper anode MFCs. (Error bars ± SD based on averages measured during stable power output in two or more separate batch experiments).

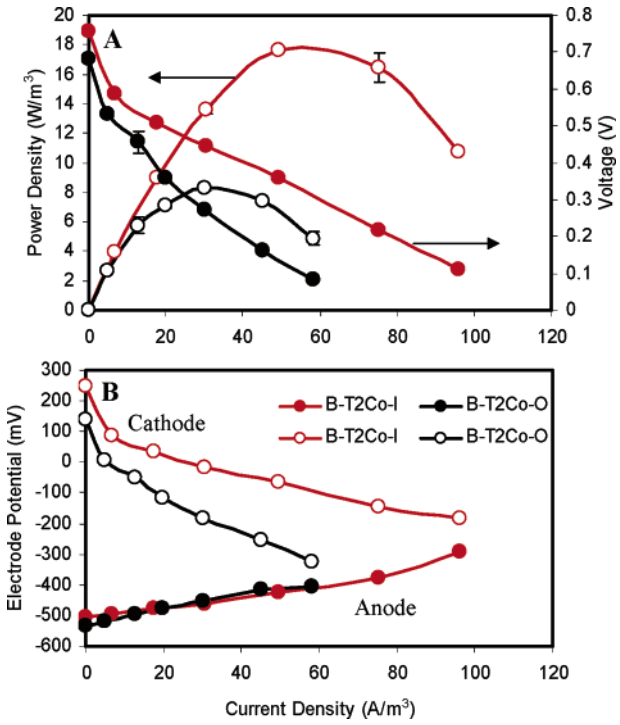

FIGURE 3. (A) Power density (open symbols), voltage (filled symbols), and (B) electrode potentials (cathode open symbols, anode filled symbols) as a function of current density (based on reactor volume) obtained by varying the external circuit resistance (40−3000 Ω) for brush anode MFCs. (Error bars ± SD based on averages measured during stable power output in two or more separate batch experiments).

As expected, all carbon paper anode MFCs had similar anode potentials at the same current (Figure 2B). The differences in power productions from these four MFC reactors were a result of the differences in cathode potentials. Tube cathode potentials were improved by adding CoTMPP as the catalyst and/or increasing the cathode surface area. With 13.5 or 27 cm^2 of surface area, the CoTMPP coated tube cathodes (C-T_1Co-I and C-T_2Co-I) achieved almost the same potentials as the carbon paper Pt cathode (C-CPt-I) over the current density range of 0−60 A/m^3.

Power Production from Tube Reactors with Brush Anodes. All of the tube reactors with brush anodes generated repeatable power cycles after ~14 batch cycles (50 mM PBS). After the buffer concentration was increased to 200 mM, a maximum volumetric power density of 17.7 ± 0.2 W/m^3 (R_{ext} = 250 Ω) was produced with two 3-cm tube cathodes inside the reactor (B-T_2Co-I, A_{cat} = 27 cm^2) (Figure 3A). The 200% increased power produced with the brush versus the carbon paper anode in the same type of tube cathode reactor (C-T_2Co-I, 8.8 ± 1.0 W/m^3) was consistent with an overall reduction in internal resistance (from 89 to 66 Ω) and a significant increase of the anode area (from 7 to 2235 cm^2). The power produced with brush anode and tube cathodes inside the reactor was also double the maximum power of 8.2 ± 0.2 W/m^3 (R_{ext} = 250 Ω) from the brush reactor with a single 6-cm tube placed outside (B-T_2Co-O, A_{cat} = 27 cm^2) (Figure 3A). The increase in power output with the tubes inside the reactor was caused by the higher cathode potentials as the brush anode potentials remained unchanged over a current range of 0−58 A/m^3 (Figure 3B). The OCP of the cathode when inside the reactor (250 ± 8 mV, vs Ag/AgCl) was 112 mV higher than when it was placed outside the reactor (138 ± 16 mV). As the current increased, the potential difference further increased to 240 mV at 58 A/m^3 (Figure 3B).

Coulombic Efficiencies Using Tube Cathodes. The CEs of all reactors were a function of current densities (Table 1; additional information in Supporting Information). With carbon paper anodes, the tube cathodes with a CoTMPP catalyst achieved CEs as high as 40%, while carbon paper cathodes with Pt (C-CPt-I) had CEs of 7−19%. Without a catalyst (C-T_1C-I), the CEs for the tube cathode reactor ranged from 18 to 22%. By using a graphite brush anode, and increasing the solution ionic strength using 200 mM PBS, the CE further increased to 52−58% when the tube was placed outside the reactor (B-T_2Co-O), and 70−74% for the tube placed inside the reactor (B-T_2Co-I).

The higher CEs obtained with tube cathode reactors were thought to be due to lower O_2 diffusion rates through the tubular ultrafiltration membrane than through the carbon paper cathode. For a clean tubular membrane, we measured an O_2 mass transfer coefficient $k = 7.8 \times 10^{-5}$ cm/s, which could result in as much oxygen transfer as 0.03 mgO_2/h into an MFC system with a tube cathode surface area of 13.5 cm^2 (C-T_1Co-I and C-T_1C-I), or 0.06 mgO_2/h for a surface area of 27 cm^2 (C-T_2Co-I, B-T_2Co-I, and B-T_2Co-O). In contrast, a carbon paper cathode of 7 cm^2 (C-CPt-I) produced an oxygen rate of 0.187 mg/h (*7*). It therefore seems likely that the higher CEs of the tube cathode system were due to the reduction in substrate lost to aerobic oxidation supported by oxygen diffusion through the cathode.

Effect of Tube Cathode Surface Area. The effect of tube cathode surface area was investigated for brush anode reactors with the tube cathodes placed inside or outside the reactor. The cathode surface areas for both configurations were increased from 27 (T_2) to 40.5 (T_3) or 54 cm^2 (T_4), by adding more 3-cm tubes inside the reactor (B-T_3Co-I and B-T_4Co-I) or extending the length of the outside tube up to 12 cm (B-T_4Co-O). For the tubes inside the reactor, the maximum power output increased with cathode surface area,

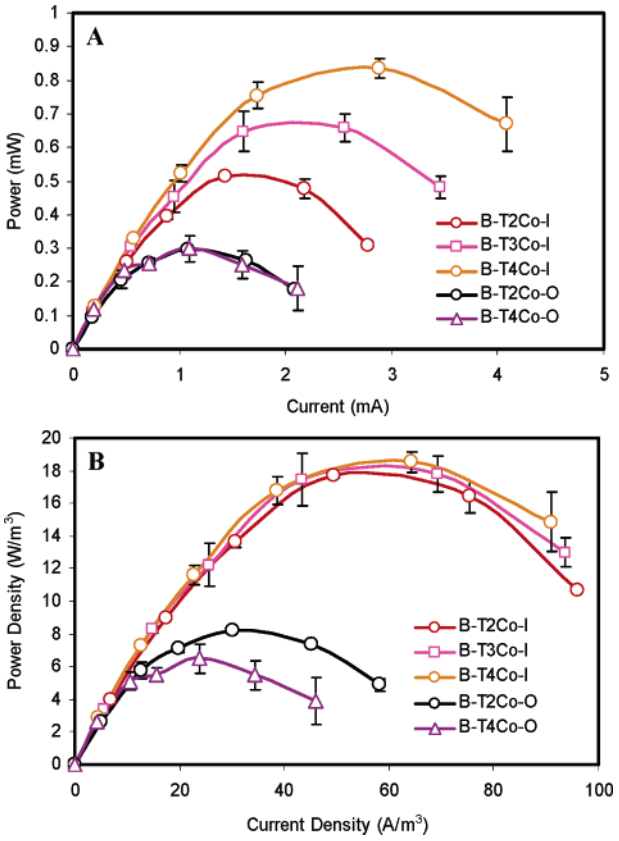

FIGURE 4. (A) Power and (B) volumetric power density as a function of the cathode surface area of tube cathode MFCs with brush anodes. (Error bars ± SD based on averages measured during stable power output in two or more separate batch experiments).

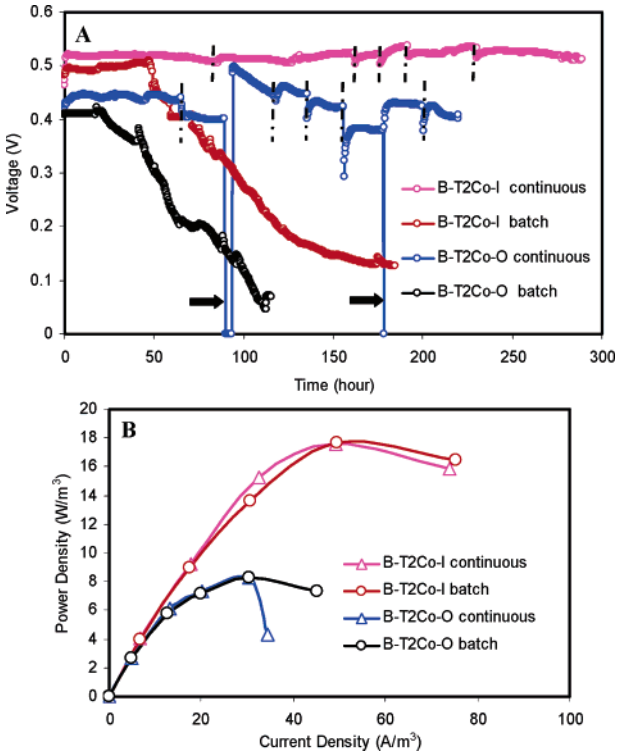

FIGURE 5. (A) Voltage as a function of time at a fixed resistance of 1000 Ω (except as noted) and (B) volumetric power density as a function of current (normalized to volume) obtained by varying the external circuit resistance (40−3000 Ω) for brush anode MFCs operated in continuous or batch mode. Vertical lines indicate where the external resistance was changed for polarization curve measurements. Arrows indicate the replacement of the tube cathode outside the reactor.

producing 0.51 mW (B-T_2Co-I), 0.66 mW (B-T_3Co-I), and 0.83 mW (B-T_4Co-I) (Figure 4A). Since the reactor volume also increased by 8 mL when adding each 3-cm tube, however, the volumetric power densities produced by these different reactors with the tubes inside the reactor were similar when normalized to volume, producing for all cases a maximum of ~18 W/m^3 (Figure 4B). When the tube was placed outside the reactor, the maximum power output was not improved with increased tube length (Figure 4A). Although both reactors produced ~0.3 mW, the longer tube cathode added 10 mL more volume than the shorter one, resulting in a decrease in volumetric power from 8.2 (B-T_2Co-O) to 6.5 W/m^3 (B-T_4Co-O) (Figure 4B).

Continuous Flow Performance of Tube Cathode Reactors. Two brush anode MFCs with the tube cathodes inside or outside the reactor were also operated in continuous flow mode. With the tubes inside the reactor (B-T_2Co-I; A_{cat} = 27 cm^2), the voltage output (520 mV at 1000 Ω) was immediately produced and was stable for more than 10 HRTs (Figure 5A). Power density curves showed that the performance was identical to that produced in fed-batch tests, resulting in a maximum power density of ~18 W/m^3 (Figure 5B).

Power density curves measured for the MFC with the tube outside the reactor were also similar for continuous and fed batch operation (Figure 5B). However, the voltage produced by this reactor (B-T_2Co-O, A_{cat} = 27 cm^2) was unstable over time, and decreased from 500 to 380 mV (1000 Ω) (Figure 5A). Over time, the catalyst layer coating on the outside of the tube gradually cracked, with visible salt accumulation on the outside of the tube. On average, the system could operate for only 100 h before the catalyst layer showed large cracks.

The effluents from both reactors operated in continuous flow mode were analyzed with a fixed external resistor of 1000 Ω. The reactor with the tube outside the MFC produced a COD removal of 53 ± 5 %, compared to 37 ± 5 % when the tubes were inside the reactor.

Internal Resistance Contributed by Tube Cathodes. The internal resistance with a flat piece of tubular membrane material (7 cm^2) placed between two carbon electrodes in a two-chamber cube reactor, was measured as $R_{int,m+}$ = 247 ± 6 Ω. When the membrane was removed, the internal resistance was $R_{int,m-}$ = 84 ± 1 Ω, which was the same as reported by Kim et al. (*24*). These resistances indicate that the proton transport resistivity of the membrane was 1141 Ω·cm^2, resulting in internal resistances of 84 Ω or 42 Ω for the 13.5 cm^2 or 27 cm^2 tubular membrane cathodes. This indicates that the membrane accounted for up to 64% of the total internal resistances of the tube cathode reactors.

Discussion

Coating tubular ultrafiltration membranes with a graphite paint and a nonprecious metal catalyst (CoTMPP) produced a maximum volumetric power density of 17.7 W/m^3, while at the same time achieving a CE of 70−74% when the cathode tube membranes were placed inside the reactor and close to the brush anode (B-T_2Co-I). This volumetric power density was greater than that produced here with a cube reactor using two carbon paper electrodes (9.9 W/m^3) and 4-cm spacing between the electrodes. The volumetric power density produced with the tube cathodes was also larger than that produced with a same type of cube reactor when a Nafion membrane was hot-pressed to a carbon cloth cathode reported by Liu et al. (262 mW/m^2, 6.6 W/m^3) (*7*). Higher power densities by tube cathode reactors were limited by the reactor internal resistance, which was measured to range

from 66 to 131 Ω. Internal resistances using ferricyanide cathode MFC systems have been equal to or lower than these values, ranging from 4−8 to 84 Ω, and resulting in power volumetric densities of 38 W/m^3 (with glucose) and 48 W/m^3 (with acetate) (*15*) to 3.1W/m^3 (with a sucrose and yeast-extract solution) (*26*).

Increasing power production in a tubular cathode MFC will require the development of tubular membranes that have lower internal resistances. It was recently shown by Kim et al. (*24*) that a Nafion membrane did not affect the internal resistance when it was placed in solution between the anode and cathode in a two-chamber cube reactor of the same type as used in this study. Thus, it is not the presence of the Nafion membrane *per se* that affected power production in the study by Liu et al. (*7*), but rather a result of the bonding of the membrane to the cathode. It was also shown by Kim et al. (*24*) that replacing the Nafion membrane with an ultrafiltration (UF) membrane significantly increased the internal resistance. Adding the UF tubular membrane used here between electrodes in that cube reactor increased the internal resistance to 247 Ω, compared to 84 Ω produced without a membrane or when using a Nafion membrane (*24*) in the same system. These results showed that the tubular membrane cathodes contributed 42 Ω (27 cm^2 membrane area) of the 66 Ω for the brush anode MFC with two tube cathodes inside the reactor and filled with 200 mM PBS, or 64% of the total internal resistance. Other types of flat UF membranes examined by Kim et al. (*24*) produced internal resistances of 1814, 98, and 91 Ω for molecular weight cut offs of 0.5, 1, and 3 K. In contrast, cation and anion exchange membranes produced 84 and 88 Ω resistances under the same conditions (*24*). These findings indicate that it will be possible to substantially improve reactor performance by developing tubular membranes that have lower internal resistances than those tested here.

The architecture of the MFC containing tube membranes will be an important factor in power generation. Comparisons of power production with the cathode tubes in different orientations (inside and outside the reactor), and with flow directed to the cathode in different ways (around the tube versus through the tube) suggests that the best anode brush and cathode tube orientation is with the brush and tube placed as closely as possible in the same chamber. The potential of the cathode with the tubes placed inside reactor was 112−240 mV higher than when the tube was outside the reactor (current range of 0−58 A/m^3). This higher voltage resulted for several reasons. First, with the tubes inside the reactor (B-T_2Co-I) there was a shorter distance between the electrodes (3 cm vs 5 cm, measured between the anode and the midpoint of the tube cathode), producing a lower internal resistance (66 ± 1 Ω versus 85 ± 8 Ω), which increased the cathode potential as previously observed (*20*). Second, when the tubes were on the inside of the reactor the catalyst was on the membrane side (polysulfone) of the tube, versus the supporting side (polyester). This difference in location could alter the effectiveness of the catalyst in terms of proton and oxygen diffusion to the catalyst surface on the supported material. Finally, we observed that when the reactor was operated in continuous flow, with the water flow directed through the tube (B-T_2Co-O), power production was not stable. Under these conditions, the catalyst layer cracked and we observed extensive salt precipitation on the outside of the tube, indicating this within-tube orientation of the flow as not a suitable reactor configuration.

The specific surface areas of the two electrodes per volume of reactor (specific surface areas) will need to be optimized. Previous findings with brush anodes suggests that anode specific surface areas in the range used here are well in excess of that needed for maximum power production (*19*). However, the same is not true for cathode surface areas as tests conducted here showed increasing cathode surface area increased power. Increasing the cathode surface area from 27 up to 54 cm^2 (from 93 to 120 m^2/m^3; B-T_2Co-I, B-T_3Co-I, B-T_4Co-I) increased the power generation by up to 63%. However, because of the large size of the cathode tubes, the power normalized to reactor volume was essentially unchanged due to the increase in reactor volume needed to accommodate the large cathodes. It was not possible with the cathode tubes used here to maintain a constant reactor volume, but in future tests with larger reactors this may be possible. In other systems this effect of cathode surface area on power has also been observed. For example, in two-bottle MFCs, it was observed that increasing the cathode surface area from 22.5 to 67.5 cm^2 (from 9 to 27 m^2/m^3) increased power output by 24% (*27*). An MFC used to generate power from domestic wastewater produced only 1.6 W/m^3 (26 mW/m^2), but that reactor had a cathode specific surface area of only 30 m^2/m^3. These specific surface areas so far tested for air cathode MFCs are well below surface areas used in membrane bioreactors of 180 to 6800 m^2/m^3 (*28*, *29*). Thus, it is likely MFC reactor performance can be increased using membranes with larger surface area to volume ratios. However, maximizing the cathode surface area is not the only challenge as membrane cost must also be considered. The tubular membranes we used here cost $350/m^2, which is less expensive than Nafion ($1400/m^2), but more expensive than other types of commercially available membranes. Thus the relative amounts of anode and cathode materials will need to be optimized based on cost and performance.

This procedure of converting conventional nonconductive ultrafiltration membranes into electrically conductive and catalytically active cathodes opens up a whole new approach toward MFC design, and it should allow easy scale up of the system when combined with the high specific surface areas of graphite brush anodes (*30*). Different types of membranes and other modifications to the conductive materials can be expected to increase power. The CoTMPP catalyst used here is indicated to be suitable for power generation, but other nonprecious catalysts should be investigated for performance and longevity in these systems. In addition, it has been recently shown by our group that a high-temperature ammonia treatment of the brush electrode can increase power production and reduce acclimation time of the MFC for power production (*19*). These and other anode treatments (*31*−*33*) could therefore be expected to improve performance of subsequent systems. The high recovery of electrons with the tube cathodes, as indicated by high CEs, the use of readily available materials, reasonable costs of these materials, and promising performance in these designs all indicate that MFCs based on these brush anodes and tube cathodes are now ready for the next level of testing in larger systems. Through the analysis of performance of these larger systems, it will be possible to evaluate the performance of the system for use as a wastewater treatment technology.

Acknowledgments

We thank D. W. Jones for help with analytical measurements, and NORIT Process Technology B.V. and X-flow B.V. (Netherlands) for providing the membranes. This research was supported by National Science Foundation Grant BES-0401885.

Supporting Information Available

Coulombic efficiencies are shown as a function of current density for different reactor configurations. This material is available free of charge via the Internet at http://pubs.acs.org.

Literature Cited

(1) Logan, B. E. Feature Article: Extracting hydrogen and electricity from renewable resources. *Environ. Sci. Technol.* **2004**, *38*, 160A−167A.

(2) Logan, B. E.; Regan, J. M. Microbial fuel cells—Challenges and applications. *Environ. Sci. Technol.* **2006**, *40*, 5172−5180.
(3) Lovley, D. R. Bug juice: harvesting electricity with microorganisms. *Nat. Rev. Microbiol.* **2006**, *4*, 497−508.
(4) Oh, S.; Min, B.; Logan, B. E. Cathode performance as a factor in electricity generation in microbial fuel cells. *Environ. Sci. Technol.* **2004**, *38*, 4900−4904.
(5) Cheng, S.; Liu, H.; Logan, B. E. Increased performance of single-chamber microbial fuel cells using an improved cathode structure. *Electrochem. Commun.* **2006**, *8*, 489−494.
(6) Gil, G.; Chang, I.; Kim, B. H.; Kim, M.; Jang, J.; Park, H. S.; Kim, H. J. Operational parameters affecting the performance of a mediator-less microbial fuel cell. *Biosens. Bioelectron.* **2003**, *18*, 327−334.
(7) Liu, H.; Logan, B. E. Electricity generation using an air-cathode single chamber microbial fuel cell in the presence and absence of a proton exchange membrane. *Environ. Sci. Technol.* **2004**, *38*, 4040−4046.
(8) Min, B.; Cheng, S.; Logan, B. E. Electricity generation using membrane and salt bridge microbial fuel cells. *Water Res.* **2005**, *39*, 1675−1686.
(9) Chaudhuri, S. K.; Lovley, D. R. Electricity generation by direct oxidation of glucose in mediatorless microbial fuel cells. *Nat. Biotechnol.* **2003**, *21*, 1229−1232.
(10) Rabaey, K.; Lissens, G.; Siciliano, S. D.; Verstraete, W. A microbial fuel cell capable of converting glucose to electricity at high rate and efficiency. *Biotechnol. Lett.* **2003**, *25*, 1531−1535.
(11) Aelterman, P.; Rabaey, K.; Pham, T. H.; Boon, N.; Verstraete, W. Continuous electricity generation at high voltages and currents using stacked microbial fuel cells. *Environ. Sci. Technol.* **2006**, *40*, 3388−3394.
(12) Rhoads, A.; Beyenal, H.; Lewandowski, Z. Microbial fuel cell using anaerobic respiration as an anodic reaction and biomineralized manganese as cathodic reactant. *Environ. Sci. Technol.* **2005**, *39*, 4666−4671.
(13) Zhao, F.; Harnisch, F.; Schröder, U.; Scholz, F.; Bogdanoff, P.; Herrmann, I. Challenges and constraints of using oxygen cathodes in microbial fuel cells. *Environ. Sci. Technol.* **2006**, *40*, 5193−5199.
(14) Liu, H.; Ramnarayanan, R.; Logan, B. E. Production of electricity during wastewater treatment using a single chamber microbial fuel cell. *Environ. Sci. Technol.* **2004**, *38*, 2281−2285.
(15) Rabaey, K.; Clauwaert, P.; Aelterman, P.; Verstraete, W. Tubular microbial fuel cells for efficient electricity generation. *Environ. Sci. Technol.* **2005**, *39*, 8077−8082.
(16) He, Z.; Wagner, N.; Minteer, S. D.; Angenent, L. T. The upflow microbial fuel cell with an interior cathode: assessment of the internal resistance by impedance spectroscopy. *Environ. Sci. Technol.* **2006**, *40*, 5212−5217.
(17) Cheng, S.; Liu, H.; Logan, B. E. Power densities using different cathode catalysts (Pt and CoTMPP) and polymer binders (Nafion and PTFE) in single chamber microbial fuel cells. *Environ. Sci. Technol.* **2006**, *40*, 364−369.
(18) Zhao, F.; Harnisch, F.; Schröder, U.; Scholz, F.; Bogdanoff, P.; Herrmann, I. Application of pyrolysed iron (II) phthalocyanine and CoTMPP based oxygen reduction catalysts as cathode materials in microbial fuel cells. *Electrochem. Commun.* **2005**, *7*, 1405−1410.
(19) Logan, B. E.; Cheng S.; Watson, V.; Estadt, G. Graphite fiber brush anodes for increased power production in air-cathode microbial fuel cells. *Environ. Sci. Technol.* **2007**, *41*, 3341−3346.
(20) Liu, H.; Cheng, S.; Logan, B. E. Power generation in fed-batch microbial fuel cells as a function of ionic strength, temperature, and reactor configuration. *Environ. Sci. Technol.* **2005**, *39*, 5488−5493.
(21) Cheng, S.; Logan, B. E. Ammonia treatment of carbon cloth anodes to enhance power generation of microbial fuel cells. *Electrochem. Commun.* **2006**, *9*, 492−496.
(22) Zuo, Y.; Maness, P-C.; Logan, B. E. Electricity production from steam exploded corn stover biomass. *Energy Fuels* **2006**, *20* (4), 1716−1721.
(23) Cheng, S.; Liu, H.; Logan, B. E. Increased power generation in a continuous flow MFC with advective flow through the porous anode and reduced electrode spacing. *Environ. Sci. Technol.* **2006**, *40*, 2426−2432.
(24) Kim, J.-R.; Cheng, S.; Oh, S.-E.; Logan, B. E. Power generation using different cation, anion, and ultrafiltration membranes in microbial fuel cells. *Environ. Sci. Technol.* **2007**, *41* (3), 1004−1009.
(25) American Public Health Association, American Water Works Association, and Water Pollution Control Federation. *Standard Methods for the Examination of Water and Wastewater*, 19th ed.; Washington, DC, 1995.
(26) He, Z.; Minteer, S. D.; Angenent, L. T. Electricity generation from artificial wastewater using an upflow microbial fuel cell. *Environ. Sci. Technol.* **2005**, *39*, 5262−5267.
(27) Oh, S.; Logan, B. E. Proton exchange membrane and electrode surface areas as factors that affect power generation in microbial fuel cells. *Appl. Microbiol. Biotechnol.* **2006**, *70*, 162−169.
(28) Water Environmental Federation. *Membrane Systems for Wastewater Treatment*; WEF: New York, 2006.
(29) American Water Works Association Research Foundation, Lyonnaise des Eaux, and Water Research Commission of South Africa. *Water Treatment Membrane Processes*; New York, 1996.
(30) Logan, B. E. Material and configuration for scalable microbial fuel cells. Provisional patent application, 2006.
(31) Park, D. H.; Zeikus, J. G. Improved fuel cell and electrode designs for producing electricity from microbial degradation. *Biotechnol. Bioeng.* **2003**, *81*, 348−355.
(32) Lowy, D. A.; Tender, L. M.; Zeikus, J. G.; Park, D. H.; Lovley, D. R. Harvesting energy from the marine sediment-water interface. II-Kinetic activity of anode materials. *Biosens. Bioelectron.* **2006**, *21*, 2058−2063.
(33) Kim, J.; Min, B.; Logan, B. E. Evaluation of procedures to acclimate a microbial fuel cell for electricity production. *Appl. Microbiol. Biotechnol.* **2005**, *68*, 23−30.

Received for review November 20, 2006. Revised manuscript received February 5, 2007. Accepted February 14, 2007.

ES0627601